REVISTA MATÉRIA V.26 N.04
ISSN 1517-7076 artigos e13086, 2021

Bacterial nanocellulose and fibroin: natural products to produce a structure membranes

Nanocelulose bacteriana e fibroína: produtos naturais para a produção de membranas estruturais

Victória Soares Soeiro[1], Louise Lacalendola Tundisi[2], Venâncio Alves Amaral[3], Fenando Batain[3], Priscila Gava Mazzola[2], Elias Basile Tambourgi[4], José Martins de Oliveira Júnior[5], Marco Vinicius Chaud[3], Denise Grotto[6], Norberto Aranha[1], Angela Faustino Jozala[1,6]

[1] University of Sorocaba, LAMINFE – Laboratory of Industrial Microbiology and Fermentation Process, SP-270, km 92,5, Zip Code 18023-000. Sorocaba/SP, Brazil
[2] University of Campinas, Faculty of Pharmaceutical Science, Rua Candido Portinari, 200, Zip Code 13083871, Campinas, SP- Brazil.
[3] University of Sorocaba, LABNUS – Laboratory of Biomaterials and Nanotechnology, University of Sorocaba, Av. 1777, Jardim Santa Cecilia. Zip Code 18078-005, Sorocaba, SP, Brazil
[4] University of Campinas, School of Chemical Engineering, Av. Albert Einstein, 500, Zip Code 13083-852, Campinas/SP, Brazil
[5] University of Sorocaba, LAFINAU – Laboratory of Nuclear Physics, SP-270, km 92,5, Zip Code 18023-000. Sorocaba/SP, Brazil
[6] University of Sorocaba, LAPETOX - Laboratory of Toxicological Research, SP-270, km 92,5, Zip Code 18023-000, Sorocaba/SP, Brazil
e-mail: angela.jozala@prof.uniso.br

ABSTRACT

Fibroin (FB) and bacterial nanocellulose (BC) are natural products, being used in biomedicine, electronics, food industries and other areas. Both show biocompatibility, able to be used for many different purposes. The blending of fibroin and bacterial nanocellulose was design to produce a biocompatible material to be applied with a medical device. For this reason, the objective of this work was to evaluate the structure properties of the blending of BC and FB. Thus, FB was extracted from *Bombyx mori* and BC was produced by fermentation process utilizing *Gluconacetobacter xylinus*. The membranes composed of BC-FB were produced by immersion contact for 24 hours, at 25°C, in 100rpm; without crosslinking agent. After the production the membrane samples were dried and characterized by Fourier transform infrared spectroscopy (FTIR spectroscopy), mechanical proprieties, swelling efficiency, scanning electron microscopy (SEM) and computerized microtomography (µCt). Results indicate that the hydrogen-bonded porous membranes obtained displayed anisiotropic, closed and interconnected porous morphology. The morphometric characteristics, which resemble a honeycomb and consist of a long structure with high connectivity and high total porosity, amplify the areas of BC-FB blend applications, with potential utilization with optoelectronic devices, in areas ranging from environmental to tissue engineering. Furthermore, the production by immersion contact will allow the upscale process and the development of green label material..

Keywords: Polymers conjugation, Membranes; Fibroin; Bacterial nanocellulose.

1. INTRODUCTION

In bioengineering, the light fibroin (FB) chain found in the silk filaments of *Bombyx mori* has low immunogenicity and low risk for acute cellular rejection. FB can induce cell growth based on its structure, tissue biocompatibility and non-cytotoxicity. The material size, chains with molecular weight in the range of 200–350 kDa, does not allow the phagocytosis, and it does not cause inflammatory reactions [1-4]. Those are important characteristics in bioengineering. Nevertheless, to solubilize the FB and prevent its premature precipi-

Autor Responsável: Victória Soares Soeiro Data de envio: 27/07/2020 Data de aceite: 18/05/2021

10.1590/S1517-707620210004.1386

tation by self-assembly, the use of harsh solvents is needed. The advantage of silk fibroin is the possibility of biochemical manipulation of its solubility by artificial induction of β-sheet formation when polyaniline is incorporated [5]. The soluble FB can also be manipulated to acquire several shapes and thickness in film, fibres, nets, scaffold, mat, threads [4, 6].

Bacterial nanocellulose is a polysaccharide produced by various microorganisms including *Agrobacterium*, *Rhizobium*, *Pseudomonas*, *Sarcina* and *Acetobacter*. Its chemical composition is similar to vegetable cellulose, but its fibers are organized in nanometric dimensions and have unique properties such as high mechanical strength, chemical stability, hydrophilicity, crystallinity, and biocompatibility. [7-9]. Bacterial nanocellulose is a material of great industrial interest, with low cost and with a variety of application, as packing, biomedical devices [11-13]. A material composed only of fibroin does not show as good mechanical properties as one with reinforcing materials [2, 13]. With this in mind, fibroin films with bacterial nanocellulose were developed in order to improve the mechanical properties of the material and amplify the application areas. For this reason, this study aimed to evaluate the structural properties of the blend composed for fibroin and bacterial nanocellulose by immersion contact.

2. MATERIAL AND METHODOLOGY

2.1 Fibroin (FB) extraction

Fibroin was extracted utilizing our research group protocol [14] where 5g of *Bombyx mori* cocoons (Bratac – Londrina/PR-Brazil) were used. The cocoons were cut and immersed in sodium carbonate solution (P.A., Anidrol – Diadema/SP-Brazil) prepared with MilliQ water 4.54g/L. The solution was kept for 35 min at 80°C for sericin and other proteins withdrawal takes place since are soluble in heated sodium carbonate solution.

After the 35 minutes, the fibers were washed three times carried out for 30 min each with 1 L of purified water on a magnetic stirrer to remove the sodium carbonate. The remaining material was dried at 50°C for 24 h. In order to dissolve the fibers and to form a fibroin suspension, a ternary solution containing calcium chloride (P.A., Anidrol– Diadema/SP-Brazil), ethanol (95%, Anidrol– Diadema/SP-Brazil) and MilliQ water (1:2:8 molar ratio) was applied. The solution was then heated at 85°C in a water bath for 20 min. Once the fibers reached full dissolution, the mixture was removed from the bath and cooled to room temperature (23 ± 2°C).

The fibroin suspension (12 mL) was placed in dialysis using a cellulose membrane with a 33 mm MWCO 12.000 Da (Sigma Aldrich). Each membrane containing the solution was immersed in 1 L of purified water under stirring for 48 h, changing the water after 24 h. The membranes were withdrawn and the solution was centrifuged twice at 20,000 rpm for 30 minutes to remove possible remaining impurities. The proteins concentration in fibroin solution, pH 7, was 1 mg/mL, a value similar to that reported in the literature, which is 10% [14]. To avoid contamination, the material was autoclaved at 121°C for 15 min and then stored at 8°C.

2.2 Bacterial nanocellulose (BC) production

Bacterial nanocellulose (BC) was produced using *Gluconacetobacter xylinus* (ATCC 53582) in 20 mL of the Hestrin & Schramm broth (20 g/L glucose, 5 g/L bacteriological peptone, 5 g/L yeast extract, 2.7 g/L anhydrous sodium phosphate, 1.5 g/L monohydrate citric acid) in an Erlenmeyer flask of 125 mL. The Erlenmeyers were kept for 4 days in static culture at 30°C, yielding 2 mm thick BC. After growth, they were washed in 2% sodium dodecyl sulfate (SDS) solution in a magnetic stirrer overnight. Afterwards, they were rinsed with distilled water until SDS removal, and immersed in 1 M NaOH solution with stirring (50 rpm) at 60ºC for 1h30. After this period, membranes were washed again until reaching neutral pH. They were packaged and autoclaved at 121°C for 15 minutes in MilliQ water, and stored at 4°C [15, 16]

2.3 Bacterial nanocellulose and fibroin membranes (BC-FB) production

The BC-FB membranes were produced by immersion contact utilizing bacterial nanocellulose (with diameter of 150 mm and thickness of 2 mm) with 20 mL of the aqueous fibroin solution (1mg/mL) in a 125 mL Erlenmeyer's flask at 25ºC, under agitation (100 rpm for 24h). After the immersion contact the BC-FB membranes were freeze for 24h in -80 ºC and then the membranes were lyophilized.

2.4 Mechanical, physical-chemical and morphometric characterization

Fourier Transform Infrared Spectroscopy (ATR-FTIR)

FTIR technique (Shimadzu, IRAffinity-1, Kyoto, Japan) was used to collect FT-IR spectra via Labs Solutions Software v.2.10. The chemical functionalities of the samples were determined by an attenuated total reflectance (ATR-8200HA) cell on the FTIR spectrophotometer over the range between 4000 and 600 cm^{-1}, resolution of 4 cm^{-1}, interval of 0.5 cm^{-1}, averaging 128 scans. To evaluate the sample uniformity three samples were analysed. The membranes samples were carefully manipulated and put on the ATR support following the protocol reported by ARAUJO *et al.* [14].

Morphometry

The pore size, porosity (%), and the interconnectivity of the porous in the membranes were evaluated by microtomography (μCT) according to our research article [12]. The membranes pictures were captured by X-Ray microtomography (Bruckermicro CT - SkyScan 1174, Kontich, Belgium), scanner resolution of the 28mM pixel, and integration time at 1.7 s. The X-rays source was 35 keV and 795 mA. The projections were taken in a range of 180° with an angular level of 1° of circumrotating. A 3D virtual models, representative of various sections of scaffolds were built, and the data was mathematically managed by CT Analyzer software, v. 1.13.5.2.2.8 [15]

Swelling efficiency

The BC-FB membrane were kept at -80°C in an ultra-freezer for 24 hours, lyophilized for 72 hours and the weight was assessed. The lyophilized sample was immersed in phosphate buffer solution at room temperature (25oC) for different lengthy: 0, 1, 2, 3, 4, 5, 6, 7, 8 and 24 hours. The swelling ratio (SR) was calculated by the equation 1 [18]:

$$SE\%=(〖BCFB〗_w-〖BCFB〗_d)/〖BCFB〗_d \times 100 \quad \textbf{(1)}$$

in which BCFBw and BCFBd are respectively the weight of the wet and dry of BC+BF membrane.

To carry out the test, the membranes were cut to approximate in 20mm of diameter, weighed and then immersed in 3ml PBS at 37°C for up to 24 hours. At different times, they were removed, and two different measurements of their capacity to retain the PBS were made. The measurement was to assesses the ability of the membrane structure as a whole (the material itself together with the pore system) to absorb PBS. For this, at each time interval, the samples were removed from PBS, shaken gently, and then weighed without dripping (W). The scaffolds were then dried at 37°C until a constant weight was reached (Wd). The percentage of fluid uptake, in both cases, was calculated as shown (Eq. (2)):

$$\text{Fluid uptake of membrane} = (W - Wd / Wd) \times 100 \quad \textbf{(2)}$$

. Each sample was measured in triplicate.

Texturometer tests

Texture profile analysis (TPA) was performed to measure the mechanical properties of sample in compression mode for elasticity, resilience and relaxation according to ALVES *et al.* [17] in a Texture Analyzer (Stable Micro Systems - TA-XT Plus, Surrey, UK), with analytical Cylindric Probe P/2 and support HDP/FS-R. The travelling arm was outfitted with a load cell of 5 Kg and the force response of the sample to the deformation imposed on it was recorded. The samples with 150 mm diameter were clamp in a jaw probe constrained to move in a direction perpendicular to the axis of traction without rotating. The test speed was set to a rate of 2 $mm.s^{-1}$ for perforation and 0.05 $mm.s^{-1}$ for resilience and elastic modulus. The Elastic (Young's) modulus was obtained by compressed until densification of the sample, and it was calculated with a strain that ranged between 0 and 5%.

Scanning Electron Microscopy morphology

The microstructure of the materials and membranes were monitored by scanning electron microscopy (SEM) and Energy Dispersive Spectroscopy (EDS) (JEOL, Model IT200). The BC, FB and BC-FB membranes were kept at -80°C in an ultra-freezer for 24 hours and lyophilized for 72 hours. The samples were previously fractured in liquid N_2 and fixed to the stub with double-sided adhesive tape. Microphotographs were taken using

electron beams with energy and acceleration voltage of 15 kV. The samples were randomly scanned and photomicrographed at magnifications x5000

3. RESULTS AND DISCUSSION

The BC-FB membranes were visually similar to a BC sample. The BC immersed in FB solution has slightly changed the macroscopic appearance of the samples (Figure 1).

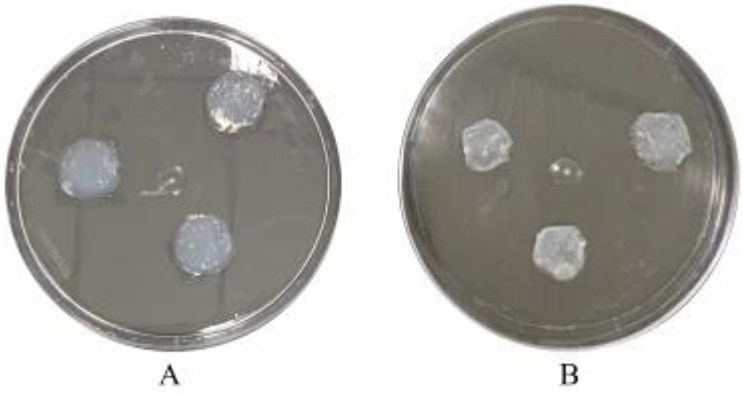

Figure 1: Photographs of bacterial nanocellulose (BC) membrane (A), BC-FB membrane.

The water swelling efficiency ratio (SR%) results for BC membranes showed the water absorption capacity around 850%, as shown in figure 2. When BC was added into FB solution, the water SR% was about 1700%, doubling the swelling capacity due to the FB hydrophilic characteristics [24]. Despite that BC can naturally hold a large amount of water and the SR is an important property involved in medical applications [27–32].

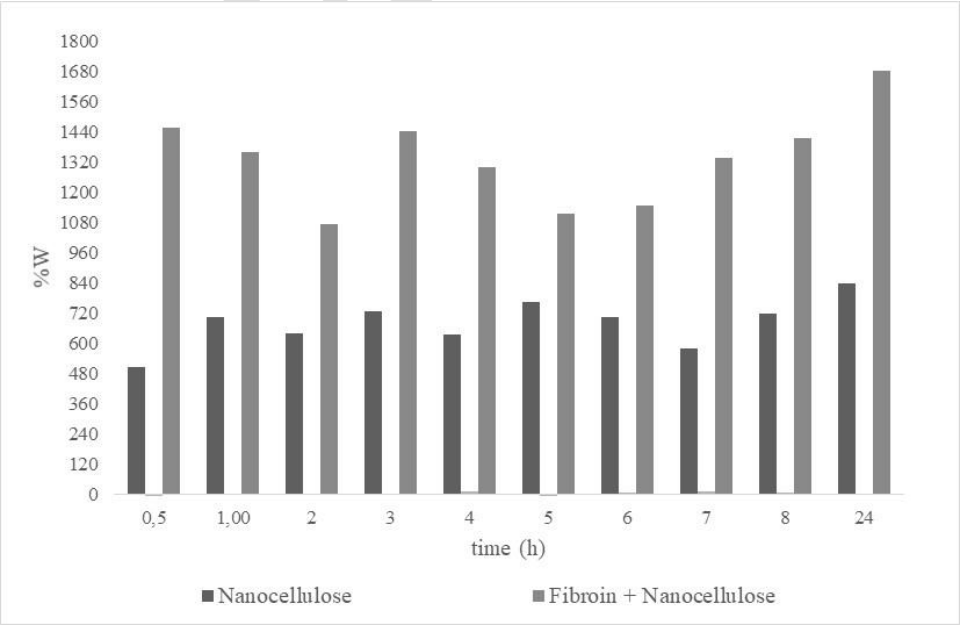

Figure 2: Swelling efficiency of BC (bacterial nanocellulose) and BC+FB (fibroin adsorbed on bacterial nanocellulose).

CHEN *et al.* [37] produced a material with fibroin aqueous solution (12%(w/v) and bacterial cellulose nanoribbon (BCNR). The materials were prepared in ratios of 0:20, 1:20, 2:20, 3:20, and 4:20 via a multi-staged freeze-drying method. They observed that water swelling efficiency ratio (SR%) increased when the material reached a ratio of 2:20. The authors have concluded the material intercalated network im-proved the SR% capacity.

MEFTAHI *et al.* [28] studied BC production in static culture medium and its properties after purification. BC simple dried membranes showed the water absorption capacity at around 450% after 196 hours immersion. The water absorption capacity was around two-times less than that obtained here for BC. We believe the reason for this difference in behaviour is that although the BC have the same production, the drying process was different.

FTIR results analyses (Figure 3) show that the chemical interaction during immersion of BC membrane into FB colloidal dispersion occur by simple σ-type polymer conjugation as there are no important band shifts after fibroin impregnation in the bacterial nanocellulose.

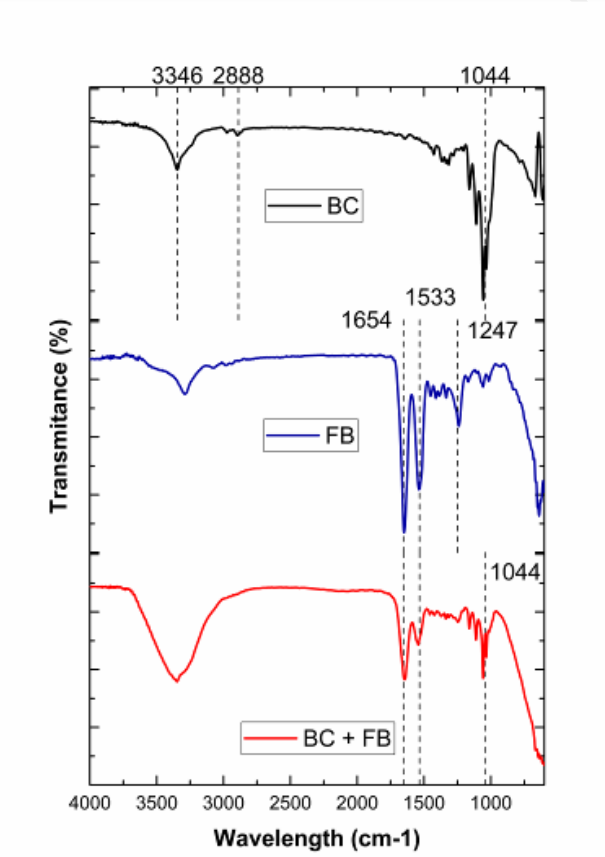

Figure 3: Fourier transform infrared spectroscopy spectra: BC (bacterial nanocellulose), FB (fibroin), BC+FB (fibroin adsorbed on bacterial nanocellulose).

The results confirm the found in FTIR spectra (Figure 3), which showed that the BC-FB interaction by hydrogen-bonded polymer conjugation. A broad band at 3500 cm^{-1} is associated with OH stretching. In addition, the positions of these bands indicate, respectively, the conformations of the protein materials (amide I, amide II, and amide III) [21, 22]. The obtained spectra of amide I (1654 cm^{-1}) is related to α-helix, β sheets, β turns and irregulars. Amide II spectra (1533 cm^{-1}) represents the angular deformation in the plane of the N-H group (60%) and by the C-N stretch (40%). The Amide III peak is a results of the combination of stretching vibrations of N - C and flexion of group C = O, and is related to the formation of β-leaf [14, 23].

The main spectra associated with BC are 3346 cm^{-1} (stretch O-H); 2888 cm^{-1} (C-H stretch), 1653 cm^{-1} (OH-deformation) and 1044 cm^{-1} (CO-deformation) [19, 24-27]. However, a peak correspondent the β-glucoside linkages between the glucose units at ~890 cm^{-1} and C−O symmetric bridge stretching of primary alcohol (1040 cm^{-1}) and C−O−C antisymmetric bridge stretching (1168 cm^{-1}). The C-H deformation for CH_3 and OH in plane bending is observed at 1340 cm^{-1}, and the band centred at 1400 cm^{-1} is related to CH_2 bend-

ing and OH plane blending. The peak at 2888 - 2895 cm^{-1} corresponds to the C-H stretching vibrations of aliphatic hydrocarbons. For FB was indicated by shifts of transmittance peaks characteristic vibrational bands at 1654 cm^{-1} (amide I: C ═ O stretching), 1533 cm^{-1} (amide II: secondary NH bending), 1230-1270 cm^{-1} (amida III: C − N stretching, and C −O flexing).

For fibroin grafting on bacterial nanocellulose (BC + FB) by immersion method, the nanocellulose bands in the region 1000 –1300 cm^{-1} are observed at the same positions although less relative intensities than BC spectra. It is possible to see amide I and amide II related of fibroin but less intense than the standard. The peaks at 2888-2895 cm^{-1} referent at C-H stretching vibrations are absent in BC + FB.

After physico-chemical analysis, the mechanical properties for BC and BC-FB membranes are explored and the results are shown in Table 1.

Table 1: Mechanical properties for BC and BC-FB membranes

PARAMETER	BC	BC-FB
Resilience (MPa)	0.71 ± 0.16	2.59 ± 0.22
Relaxation (MPa)	1.49 ± 0.05	1.86 ± 0.33
Young's modulus (MPa)	0.131 ± 0.007	0.113 ± 0.006

The presence of fibroin increased the membrane capacity to absorb energy when deformed (resilience) by compression. The relaxation reflects the induced stress as functions of time for BC and for the BC-FB polymeric membrane, and it helps to understand solvent transport as kinetics hydration, water permeation and pervaporation behaviours. The relaxation mechanism is essential to effective design the biomedical membrane, especially for dressing. The stress generated on BC-FB membranes was less than on BC membranes, due to stickiness of the membrane imposed by fibroin chain. For BC-FB membranes, a lower value in Young's modulus has been observed due to the presence of fibroin, that it is related with random coil conformation (Fibroin I), which derives from processing transition in the secondary structural from β-sheet to random coil molecular conformation state [31, 32].

It is possible to improve mechanical properties of fibroin as showed by LONG *et al*. [33] when studied silk fibroin and collagen-based membrane to repair corneal tissues and observed the improvement of optical and mechanical properties of biomaterial when fibroin was added to the samples.

WANG *et al*., [34] in order to prepared materials suitable for tissue engineering concluded when FB films were also prepared with polyethylene glycol, the samples presented greater flexibility compared to films composed of pure fibroin.

The mechanical properties of biomaterials are used as a guide to select its application. Highly resilient materials have high yield strength and low Young´s modulus and this ability makes them ideal for bone tissue material [32, 34]. NOISHIKI *et al.* [35] studied films composed of FB and cellulose fibers and the results showed improved mechanical resistance. In our study, we observed the same material behaviour when FB was added to BC as the authors above [19, 24, 32, 34, 35], which means the mechanical properties were improved.

Besides the improvement of the mechanical properties, another remarkable fact is the structure with randomly distributed pores that is formed when BC and FB are mixed (Figure 4).

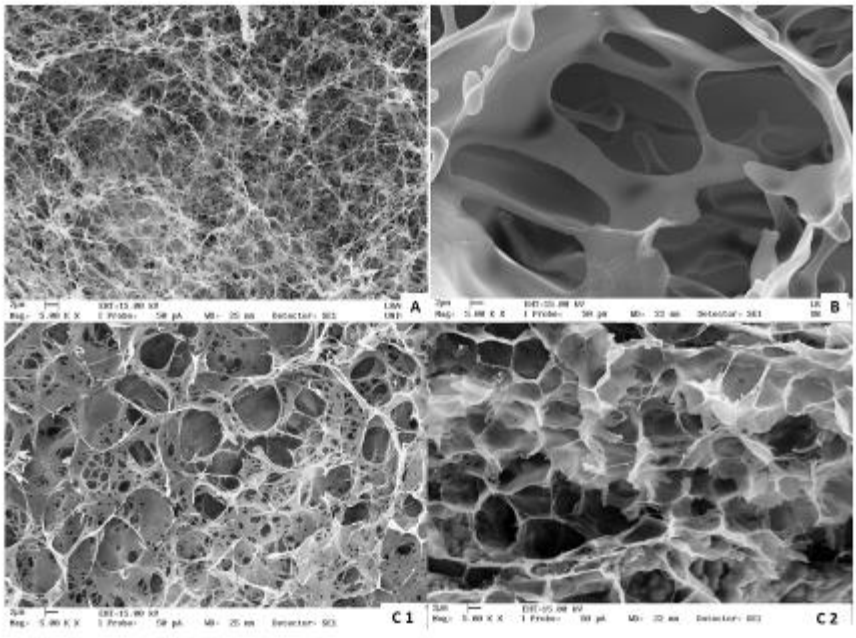

Figure 4: Scanning Electron Microscopy (SEM) microphotographs. In A, Bacterial Nanocellulose (BC); in B, Fibroin (FB) and in C1 and C2, BC-FB membranes frontal and lateral. SEM images were obtained using an accelerating voltage of 15 kV Magnification 5.00 KX and scale of 2µm.

The structure resembles a honeycomb, and a similar structure was observed by CHEN *et al.* [32]. However, the authors prepared silk FB and BC nanoribbon composite scaffolds utilizing a multi-staged freeze-drying method.

Therefore, the incorporation of FB makes the membrane more anisotropic, generating a different elasto-plastic behaviour and allowing the application in medical and pharmaceutical areas, tissue engineering and electronics [37, 38].The quantitative results of the organized structure were confirmed by X-Ray microtomography assay, presented in Table II. The pores were interconnected and distributed throughout the sample and open porosity ranged from 79.2 to 88.5%, as shown in Table II. The BC structure has a lower degree of anisotropy (DA) than the BC-FB membrane. When FB was added to BC, a 49.5% increase in DA was obtained. The parameters were analysed by 3D virtual models, representative of various sections of scaffolds were built, and the data was mathematically managed by CT Analyzer software, v. 1.13.5.2.2.8.

Table 2: X-ray microtomography parameters for samples of Bacterial nanocellulose (BC) and BC and Fibroin (BC-FB) membrane

Parameter	BC-FB	BC
Connectivity	58841 ± 2942	22421 ± 1121
Degree of anisotropy	0.794 ± 0,04	0.692 ± 0,035
Total porosity (%)	88.52 ± 4.43	79.15±3.96
Open porosity (%)	88.51± 4.43	79.15±3.96
Volume of open pore space (cm3)	489.49±24.47	237.47±11.87

*standard deviation SD ±5% ** data was mathematically managed by CT Analyzer software, v. 1.13.5.2.2.8

Although the BC already has a porous structure, when FB was added the volume was altered. Probably, because it was created a membrane with more elongated structed. This is can explain through the Structure Model Index (SMI), parameter indicates the presence of elongated or plate-like structures, data was mathematically managed by CT Analyzer software, v. 1.13.5.2.2.8. A plate-only structure has an SMI of 0 while if the structure is elongated, rod-like, the SMI value is 3 [35]. The BC-FB membrane showed high SMI value compared to the BC sample, indicating a membrane with more elongated structure. Moreover, the FB loaded in the BC structure showed an increase in the Fragmentation index, confirming the results of high connectivity between the structures. Connectivity is a geometric property that provides information about the structure of empty space [38, 39].

4. CONCLUSION

The results indicated the work reach the target of the developing a BC-FB membrane.. Blending of fibroin and bacterial nanocellulose led to membranes with improved mechanical and chemical properties, making them a viable option for different applications, as scaffolds, biomaterial or packaging.

The images observed showed the structure resembling a honeycomb, with a long structure, high connectivity and high total porosity. Since the structure is essential for materials, the BC-FB membrane could be exploited in other applications such as filter membranes or bone regeneration.

Additionally, the membrane production by immersion did not use hazardous substances, promoting an environmental-friendly material and reducing costs.

5. ACKNOWLEDGMENTS

The authors would like to acknowledge the Denicesar A. Baldo for the technical assistance for the safe operation of equipment and softwares.

6. BIBLIOGRAPHY

[1] CHOUHAN, D., MANDAL, B.B. "Silk biomaterials in wound healing and skin regeneration therapeutics: From bench to bedside", *Acta Biomaterialia*, 2019.

[2] ALTMAN, G.H., DIAZ, F., JAKUBA, C., *et al.* "Silk-based biomaterials", *Biomaterials*, v. 24, n. 3, pp. 401-416, 2003.

[3] NGUYEN T.P., NGUYEN Q.V., NGUYEN V-H. "Silk fibroin-based biomaterials for biomedical applications: a review", *Polymers (Basel)*, v. 11, n. 12, pp. 1933, 2019.

[4] GE, Z., YANG, Q., XIANG, X., *et al.* "Assessment of silk fibroin for the repair of buccal mucosa in a rat model", *International journal of oral and maxillofacial surgery*, v. 41, n. 5, pp. 673-680, 2012.

[5] ALVES, T.F., ARANHA, N., CHAUD, M.V. "Mechanical stress and thermal treatments induced alpha-helix to beta-sheet transition in silk fibroin films", *International Journal of Drug Research and Technology*, v. 8, n. 3, pp. 149-157, 2018.

[6] WANG, X., YUCEL, T., LU, Q., *et al.* "Silk nanospheres and microspheres from silk/pva blend films for drug delivery", *Biomaterials*, v. 31, n. 6, pp. 1025-1035, 2010.

[7] PANESAR, P.S., CHAVAN, Y.V, BERA, M.B., *et al.* "Evaluation of Acetobacter strain for the production of microbial cellulose", *Asian J. Chem*, v. 21, n. 10, pp. 99-102, 2009.

[8] DUFRESNE, A. "Nanocellulose Processing Properties and Potential Applications", *Current Forestry Reports*, v. 5, pp. 76-89, 2019.

[9] JACEK, P., RYNGAJLLO, M., BIELECKI, S. "Structural changes of bacterial nanocellulose pellicles induced by genetic modification of *Komagataeibacter hansenii* ATCC 23769". *Appl Microbiol Biotechnol*, v. 103, pp. 5339-5353, 2019.

[10] BERNDT, S., WESARG, F., WIEGAND, C., *et al.* "Antimicrobial porous hybrids consisting of bacterial nanocellulose and silver nanoparticles", *Cellulose*, v. 20, n. 2, pp. 771-783, 2013.

[11] DE OLYVEIRA, G.M., COSTA, L.M.M., BASMAJI, P., *et al.* "Bacterial nanocellulose for medicine regenerative", *Journal of Nanotechnology in Engineering and Medicine*, v. 2, n. 3, p. 34001, 2011.

[12] JOZALA, A.F., DE LENCASTRE-NOVAES, L.C., LOPES, A.M., *et al.* "Bacterial nanocellulose pro-

duction and application: a 10-year overview", *Applied Microbiology and Biotechnology*, v. 100, n. 5, pp. 2063–2072, 2016.

[13] AMARAL, T.S. "Nanocompósitos multifuncionas de fibroína reforçados com biocelulose", 2013.

[14] ARAÚJO, L.C.P., OLIVEIRA JÚNIOR, J.M., ARANHA, N. "Synthesis and characterization of fibroin scaffolds". *Matéria (Rio de Janeiro)*, v. 23, n. 4, 2018.

[15] JOZALA, A.F., PÉRTILE, R.A.N., DOS SANTOS, C.A., *et al*. "Bacterial cellulose production by *Gluconacetobacter xylinus* by employing alternative culture media", *Applied Microbiology and Biotechnology*, v. 99, n. 3, pp. 1181-1190, 2014.

[16] ATAIDE, J.A., CARVALHO, N.M., REBELO, M.D.A., *et al*. "Bacterial Nanocellulose Loaded with Bromelain: Assessment of Antimicrobial, Antioxidant and Physical-Chemical Properties", DOI: 10.1038/s41598-017-18271-4.*Scientific Reports*, v. 7, n. 1, pp. 2-10, 2017.

[17] ALVES, T. *et al*. "Formulation and evaluation of thermoresponsive polymeric blend as a vaginal controlled delivery system". *Journal of Sol-Gel Science and Technology*, v. 86, n. 3, p. 536-552, 2018.

[18] LIN, W-C, *et al*. "Bacterial cellulose and bacterial cellulose-chitosan membranes for wound dressing applications". *Carbohydrate polymers*, v. 94, n. 1, pp. 603-611, 2013.

[19] ALVES, T., SOUZA, J., AMARAL, V., *et al*.. "Biomimetic dense lamellar scaffold based on a colloidal complex of the polyaniline (PANi) and biopolymers for electroactive and physiomechanical stimulation of the myocardial", *Colloids and Surfaces A:* Physicochemical and Engineering Aspects, v. 579, n. July, 2019.

[20] GHOLIPOURMALEKABADI, M., SAPRU, S., SAMADIKUCHAKSARAEI, A., *et al*. "Silk fibroin for skin injury repair: Where do things stand?", *Advanced Drug Delivery Reviews*, 2019.

[21] WULANDARI, W.T., ROCHLIADI, A., ARCANA, I.M. "Nanocellulose prepared by acid hydrolysis of isolated cellulose from sugarcane bagasse", *IOP Conference Series: Materials Science and Engineering*, v. 107, n. 1, 2016.

[22] MAO, K.L., FAN, Z.L., YUAN, J.D., *et al*. "Skin-penetrating polymeric nanoparticles incorporated in silk fibroin hydrogel for topical delivery of curcumin to improve its therapeutic effect on psoriasis mouse model", *Colloids and Surfaces B: Biointerfaces*, v. 160, pp. 704-714, 2017.

[23] LU, Q., WANG, X., LU, S., *et al*. "Nanofibrous architecture of silk fibroin scaffolds prepared with a mild self-assembly process", *Biomaterials*, v. 32, n. 4, pp. 1059-1067, 2011.

[24] LU, S., LI, J., ZHANG, S., *et al*. "The influence of the hydrophilic-lipophilic environment on the structure of silk fibroin protein", *Journal of Materials Chemistry B*, v. 3, n. 13, pp. 2599–2606, 2015

[25] JACEK, P., KUBIAK, K., RYNGAJŁŁO, M., *et al*. "Modification of bacterial nanocellulose properties through mutation of motility related genes in Komagataeibacter hansenii ATCC 53582", *New Biotechnology*, v. 52, n. May, pp. 60-68, 2019.

[26] MONIRI, M., MOGHADDAM, A. B., AZIZI, S., *et al*. "Production and status of bacterial cellulose in biomedical engineering", *Nanomaterials*, v. 7, n. 9, pp. 1-26, 2017.

[27] MULAKKAL, M.C., TRASK, R.S., TING, V.P., *et al*. "Responsive cellulose-hydrogel composite ink for 4D printing", *Materials and Design*, v. 160, pp. 108-118, 2018.

[28] UL-ISLAM, M., KHAN, T., PARK, J.K. "Water holding and release properties of bacterial cellulose obtained by in situ and ex situ modification", *Carbohydrate Polymers*, v. 88, n. 2, pp. 596-603, 2012.

[29] MEFTAHI, A., KHAJAVI, R., RASHIDI, A., *et al*. "Effect of Purification on Nano Microbial Cellulose Pellicle Properties", *Procedia Materials Science*, v. 11, pp. 206-211, 2015.

[30] OLIVEIRA BARUD, H.G., BARUD, H.D.S., CAVICCHIOLI, M., *et al*. "Preparation and characterization of a bacterial cellulose/silk fibroin sponge scaffold for tissue regeneration", *Carbohydrate Polymers*, v. 128, pp. 41-51, 2015.

[31] WANG, K., MA, Q., ZHANG, Y.M., *et al*. "Preparation of bacterial cellulose/silk fibroin double-network hydrogel with high mechanical strength and biocompatibility for artificial cartilage", *Cellulose*, v. 27, n. 4, pp. 1845-1852, 2019.

[32] QI, Y., WANG, H., WEI, K., *et al*. "A review of structure construction of silk fibroin biomaterials from single structures to multi-level structures", *International Journal of Molecular Sciences*, v. 18, n. 3, 2017.

[33] LONG, K., LIU, Y., LI, W., *et al*. "Improving the mechanical properties of collagen-based membranes using silk fibroin for corneal tissue engineering", *Journal of Biomedical Materials Research - Part A*, v. 103, n. 3, pp. 1159-1168, 2015.

[34] WANG, Y., ZHENG, Z., CHENG, Q., *et al*. "Ductility and Porosity of Silk Fibroin Films by Blending with Glycerol/Polyethylene Glycol and Adjusting the Drying Temperature", *ACS Biomaterials Science and Engineering*, v. 6, n. 2, pp. 1176-1185, 2020.

[35] CHOCHOLATA, P., KULDA, V., BABUSKA, V. "Fabrication of scaffolds for bone-tissue regeneration", *Materials*, v. 12, n. 4, 2019.

[36] NOISHIKI, Y., NISHIYAMA, Y., WADA, M., *et al*. "Mechanical properties of silk fibroin–microcrystalline cellulose composite films", *Journal of Applied Polymer Science*, v. 86, n. 13, pp. 3425-3429, 2002.

[37] CHEN, J., ZHUANG, A., SHAO, H., *et al*. "Robust silk fibroin/bacterial cellulose nanoribbon composite scaffolds with radial lamellae and intercalation structure for bone regeneration", *Journal of Materials Chemistry B*, v. 5, n. 20, pp. 3640-3650, 2017.

[38] LIEB-LAPPEN, R.M., GOLDEN, E.J., OBBARD, R.W. Metrics for interpreting the microstructure of sea ice using X-ray micro-computed tomography. *Cold Regions Science and Technology*, v. 138, pp. 24-35, 2017.

[39] LIM, K.S., BARIGOU, M. "X-ray micro-computed tomography of cellular food products", *Food Research International*, v. 37, n. 10, pp. 1001-1012, 2004.

ORCID

Victória Soares Soeiro https://orcid.org/0000-0002-6890-8109
Louise Lacalendola Tundisi https://orcid.org/0000-0002-3374-6103
Venâncio Alves Amaral https://orcid.org/0000-0002-4617-2014
Fenando Batain https://orcid.org/0000-0003-1822-0944
Priscila Gava Mazzola https://orcid.org/0000-0002-3795-8189
Elias Basile Tambourgi https://orcid.org/0000-0002-4734-9723
José Martins de Oliveira Júnior https://orcid.org/0000-0001-6435-1908
Marco Vinicius Chaud https://orcid.org/0000-0003-3618-8415
Denise Grotto https://orcid.org/0000-0002-8782-0436
Norberto Aranha https://orcid.org/0000-0003-1954-377X
Angela Faustino Jozala https://orcid.org/0000-0002-3763-5451